PAN POLSKA AKADEMIA NAUK

METROLOGY AND MEASUREMENT SYSTEMS

Index 330930, ISSN 0860-8229
www.metrology.pg.gda.pl

M&MS

NOISE MEASUREMENTS OF RESISTORS WITH THE USE OF DUAL-PHASE VIRTUAL LOCK-IN TECHNIQUE

Adam Witold Stadler[1)], Andrzej Kolek[1)], Zbigniew Zawiślak[1)], Andrzej Dziedzic[2)]

1) Rzeszów University of Technology, Department of Electronics Fundamentals, Powstańców Warszawy 12, 35-959 Rzeszów, Poland (✉ astadler@prz.edu.pl, +48 17 865 1279, akoleknd@prz.edu.pl, zawislak@prz.edu.pl)
2) Wrocław University of Technology, Faculty of Microsystem Electronics and Photonics, Wybrzeże Wyspiańskiego 27, 50-370 Wrocław, Poland (Andrzej.Dziedzic@pwr.edu.pl)

Abstract

Measurement of low-frequency noise properties of modern electronic components is a very demanding challenge due to the low magnitude of a noise signal and the limit of a dissipated power. In such a case, an ac technique with a lock-in amplifier or the use of a low-noise transformer as the first stage in the signal path are common approaches. A software dual-phase *virtual lock-in* (VLI) technique has been developed and tested in low-frequency noise studies of electronic components. VLI means that phase-sensitive detection is processed by a software layer rather than by an expensive hardware lock-in amplifier. The VLI method has been tested in exploration of noise in polymer thick-film resistors. Analysis of the obtained noise spectra of voltage fluctuations confirmed that the $1/f$ noise caused by resistance fluctuations is the dominant one. The calculated value of the parameter describing the noise intensity of a resistive material, $C = 1 \cdot 10^{-21}$ m^3, is consistent with that obtained with the use of a dc method. On the other hand, it has been observed that the spectra of (excitation independent) resistance noise contain a $1/f$ component whose intensity depends on the excitation frequency. The phenomenon has been explained by means of noise suppression by impedances of the measurement circuit, giving an excellent agreement with the experimental data.

Keywords: $1/f$ noise, polymer thick-film resistor, low-frequency noise measurements, virtual lock-in.

1. Introduction

Modern electronic components and materials are subject of continuous improvements by means of optimizing their internal structure or applying new materials, which is stimulated by the RoHS directive [1] restricting the use of some elements, *e.g.* lead and cadmium, as well as modifying or developing new ways of manufacturing, in order to obtain cheap and reliable small-size components. Examples of new materials are Pb-free solder alloys [2] for the interconnection technology in electronic printed circuit boards and modules, and Pb/Cd-free systems of compatible conductive and resistive pastes for the thick-film technology [3, 4]. In specialized electronics, the reliability and quality of the components belong to the key parameters. It is just the low-frequency noise that is commonly considered as the indicator of the quality and reliability of a device since there is a relationship between the reliability/quality and noise that has been shown experimentally [5–9]. It is not so surprising, taking into account that noise, measured as the power spectral density of fluctuations of examined quantity on terminals of a tested device, relates strongly to inhomogeneity of its internal structure. Hence, it is very important to carefully select materials of high quality for production of low-noise and reliable electronic components.

In this work, we focus on experimental studies of the low-frequency noise in modern, small-size polymer thick-film resistors. The main difficulty concerned with noise measurements is

Article history: received on May 11, 2015; accepted on Oct. 15, 2015; available online on Dec. 07, 2015; DOI: 10.1515/mms-2015-0051.

a small area of a resistive layer which limits the amount of dissipated power. In order to improve the sensitivity of a measurement setup, a transformer is often used as the first stage of the signal path [10]. However, there are several disadvantages of the method: (*i*) the need for rejection of a dc offset, which implies measurements in a balanced dc bridge, (*ii*) the – depending on the transformer, but generally – rather narrow frequency band of observation, (*iii*) the transfer function of the signal path strongly depends on the source (*i.e.* sample) resistance, which makes the calibration of each sample necessary. Therefore, in this work we consider an ac method of noise measurements, which is free from the above disadvantages, and additionally makes it possible to obtain spectra at an extremely low frequency, which is not available in a dc method due to an ac coupling in the signal path and contribution of the amplifier noise. In the ac technique the low-frequency spectrum of resistance fluctuations, originated in the tested device, excited by an ac signal, is shifted to the side-bands around the carrier (exciting) frequency as a result of modulation. Furthermore, the contribution of the amplifier noise into the system noise may be optimized by careful selection of the value of the carrier frequency. Next, the demodulation is usually carried out in a lock-in amplifier by the phase-sensitive detection. The idea of the method has been described and analysed in [11]. The method occurred to be helpful in noise exploration at low temperature [12], down to 0.3 K. Moreover, using the ac method, either the background and total noise [11] or the excess noise [13] is directly accessible at the output, depending on phase angles used for the phase-sensitive detection. Although, in [12] a standard, *i.e.* hardware, lock-in amplifier was employed for the demodulation, in this work we show a software solution of the in-phase ('X') and out-of-phase ('Y', the quadrature component) detection, *i.e.* a virtual lock-in (VLI). Despite a lock-in technique is widely used in many research methods, there are only a few published papers that describe usefulness of the virtual lock-in [14–16] and none of them considers the use of VLI in noise exploration or multichannel detection at different sets of phase angles.

2. Virtual lock-in technique

The measurement setup developed for measurements of noise in resistive electronic components is shown in Fig. 1. It consists of a typical ac Wheatstone bridge driven by a remote controlled sinusoidal generator of high precision and stability. The bottom arms of the bridge are created by a pair of the samples R_S with matched resistance, while the upper arms contain the noiseless wire-wound ballast resistors R_B ($R_B \rangle\rangle R_S$) and additional components (omitted in the circuit of Fig. 1 for clarity) inserted for balancing the bridge.

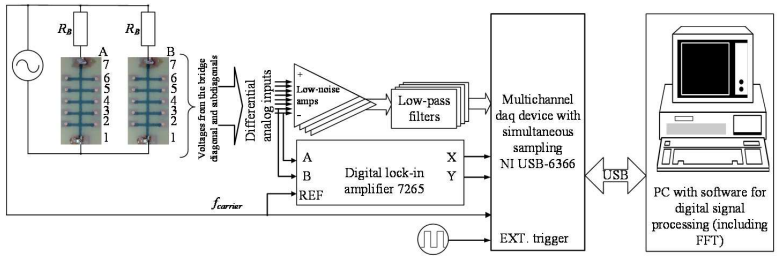

Fig. 1. The setup for measurements of noise in resistors with the use of a virtual lock-in technique.

The voltage signals from the bridge diagonal, $V_{(7-7)}$, and its sub-diagonals, $V_{(x-x)}$, where $x = 2, 3, \ldots 6$ is the side terminal, are connected to low-noise differential preamplifiers (5186 from Signal Recovery) followed by low-pass filters. Additional signal paths consisting of amplifiers followed by low-pass (anti-aliasing) filters are needed only for correlation measurements using different pairs of voltages taken from the bridge diagonal and its sub-

diagonals. Next, the signals are coupled to a multichannel data acquisition (daq) device with simultaneous sampling.

The bridge was supplied with a sinusoidal signal of frequency around 1 kHz. An additional digital lock-in amplifier (model 7265 from Signal Recovery), whose X (in-phase), and Y (quadrature) outputs were also attached to the daq device, was used for verification of the VLI results. In order to precise control the sampling frequency, an external source was used. Both ac signals, one exciting the bridge and the other triggering the daq device, were produced by a 2-channel signal generator with extended stability (model 33512B from Keysight Technology).

The software layer running on a PC takes care of (*i*) continuous acquisition of consecutive time records from the daq module, (*ii*) real-time digital signal processing (calculation of waveforms, spectra and/or cross-spectra using the FFT algorithm, phase-sensitive detection), (*iii*) presentation of the results in a graphical form on the PC screen during the experiment, (*iv*) recording data in files for further analysis, and (*v*) controlling the auxiliary equipment (digital voltmeters, a temperature controller/monitor, and a signal generator) via the GPIB interface [17]. In a dc method, the power spectral density S_V of voltage fluctuations for both biased and unbiased ($V = 0$) samples has to be obtained in separate experiments in order to get the excess noise:

$$S_{Vex} = S_V - S_{V=0}, \tag{1}$$

which is the subject of interest. The background noise, $S_{V=0}$, consists of (*i*) the thermal noise of the bridge and (*ii*) the amplifier noise. However, in the ac technique it is possible to obtain both S_V and $S_{V=0}$ simultaneously, calculating the spectra S_V^0 and S_V^{90} of signals detected at the phase angles 0° and 90°, respectively [11], *e.g.* using a dual-phase lock-in amplifier. Furthermore, calculating the cross-spectrum, S_{VV}^{45}, of signals detected at the phase angles +45° and –45° referenced to the signal driving the bridge, one may obtain directly [13]:

$$S_{Vex} = 2\mathrm{Re}(S_{VV}^{45}). \tag{2}$$

Both methods have been implemented and tested in the developed VLI.

It is worth to note, that in our configuration of the bridge (Fig. 1), the voltage from the bridge diagonal includes fluctuations originated in both samples. Hence, S_V observed on the bridge diagonal is the doubled S_V of one sample, assuming that (*i*) both samples have been carefully selected with matched resistance and have the same statistical properties, (*ii*) the bridge is balanced and therefore the ac current I (rms value) flowing through the samples is the same. Thus, $S_{V(7-7)} = 2S_{V(7-1)}$, where $S_{V(7-1)}$ is the power spectral density of voltage fluctuations in one sample.

3. Experiment

As the subject of studies a pair of polymer thick-film resistors (PTFRs), with matched resistance, prepared on the same substrate, has been taken. Resistive layers of PTFRs have been made of ED7100_200Ω – carbon-based composition from Electra Polymers Ltd on FR-4 laminate. ED7100 is a commercial ink – ElectraΩd'or™, based on epoxy resin (200 Ω/□, fillers: carbon black and graphite powders). FR4 Laminate Sheet is a glass fabric reinforcement in an epoxy resin binder. It is the most versatile laminate with an extremely high mechanical strength, good dielectric loss properties, and good electric strength properties under both dry and humid conditions – and therefore very often used on an industrial scale for the production of printed circuit boards. Polymer thick resistive films have been screen-printed on bare Cu contacts. The samples have been prepared as multi-terminal PTFRs in which the rectangular resistive layer (length L = 15 mm, width w = 0.5 mm and thickness d = 20 μm) terminated on the opposite

sides with the current terminals (see Fig. 1). Additional, equally spaced along the layer, voltage probes have been formed for detailed examinations. Such a shape of samples has been already used in the previous experiments [18]. The resistance of the selected samples was $R_S \approx 11.1$ kΩ.

Noise measurements have been carried out at the room temperature, $T = 300$ K. The carrier frequency, $f_{carrier}$, of a sinusoidal waveform (exiting the bridge) ranged from 325 Hz to 50025 Hz, while the bandwidth of the preamplifiers was 1 MHz. The sampling frequency, f_s, varied from 32 kHz to 512 kHz, the record duration, T, ranged from 4 s to 128 s and the number of samples per record, $N_s = Tf_s$ (N_s ranged from 2 M to 8 M samples), were selected so as to hold $f_s/f_{carrier} > 10$. However, there are several important technical limitations, that had to be taken into account, like the maximal sampling frequency accepted by the DAQ device ($f_{smax} = 2$ MHz) and a long time of FFT calculations for a large number N_s. The latter limits the minimal record duration, especially in the case of large N_s.

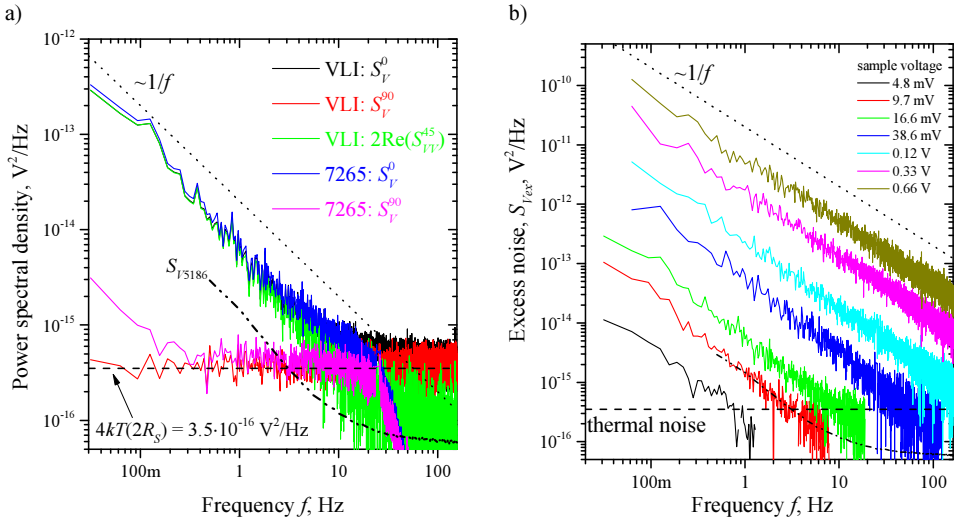

Fig. 2. a) Comparison of the noise spectra obtained in different ways at the sample voltage 16.6 mV. The dotted (pure $1/f$ noise) and dashed (thermal noise) lines have been added for reference. b) The selected excess noise spectra from VLI, *i.e.* 2Re(S_{VI}^{45}), for different sample voltages. The dash-dot-dot line is the plot of the amplifier noise.

The average spectra ($N_{av} = 20$) of voltage fluctuations, taken from the bridge diagonal, detected by the VLI and the traditional lock-in amplifier have been compared in the plot of Fig. 2a (solid lines). In fact, the respective spectra obtained with the use of the hardware lock-in amplifier (labelled "7265" in the plot's legend) and those obtained with the VLI are almost identical, making lines overlap each other. However, for the frequency above 25 Hz the rejection by the 7265 internal filter is apparent. It is worth to note, that all spectra shown in Fig. 2a were calculated from the same time records. The obvious advantage of the VLI is that the detection for different sets of phase angles is carried out on the same time records, which is impossible in a single standard lock-in amplifier. Additionally, the power spectral density of thermal noise $4kT(2R_S) = 3.5{\cdot}10^{-16}$ V²/Hz, where k is the Boltzmann constant and T – the ambient temperature, calculated for the whole bridge resistance ($2R_S$), has been plotted for reference (dashed line). Another, the dash-dot-dot line, labelled S_{V5186}, which is the plot of the amplifier noise (model 5186 from Signal recovery) referred to the input, has been added to give an imagination about the noise properties of the signal path.

4. Noise of polymer thick-film resistors

Looking at the collection of spectra shown in Fig. 2b it is apparent that the $1/f$ noise is the dominant noise component. Hence, the product of frequency and excess noise averaged over the frequency band Δf, $< f S_{Vex} >_{\Delta f}$, is a convenient measure of noise intensity. Its square dependence on the sample voltage, shown in Fig. 3a (open symbols), is the evidence that the observed noise is caused by resistance fluctuations. The solid line is the approximation of the noise intensity for the frequency band 1–10 Hz with the squared voltage. The data from measurements with a dc method [17] (solid symbols) have been added for comparison. Both ac and dc methods give consistent results.

The quadratic dependence of noise intensity on the sample voltage is the basis for evaluation of the material noise intensity, C – the parameter describing noise properties of the material itself – which is independent of the frequency, sample volume Ω, and voltage V:

$$C = <f S_{Vex}>_{\Delta f} V^{-2}\Omega. \tag{3}$$

It is worth to note, that in our experiment S_{Vex} is obtained for the voltage signal taken from the bridge diagonal, which gathers fluctuations from both samples, and therefore the voltage V and the volume Ω in the general definition (3) should be substituted by the voltage across both samples connected in serial, $V = 2V_{(7–1)}$, and the doubled volume of the single sample, respectively. The value $C = 1 \cdot 10^{-21}$ m^3 obtained for the studied samples has been found to be in a good agreement with $8.2 \cdot 10^{-22}$ m^3 obtained with a dc method [17], confirming that both methods give consistent results (see Fig. 3a).

The parameter C describes the noise properties of a resistive material itself, and therefore may be used for comparison of noise properties of bulk and layered materials. Another advantage of the parameter C [m^3] is that it enables calculation of measurable quantities, like S_V or $S_R = S_V/I^2$, provided that the geometrical sizes of the samples and the bias (voltage or current) are known. However, C strongly depends on the free carrier concentration in the sample. In view of the experiments on photoconductive and volume scaling, it turns out that the factor $1/N$ is crucial [19, 20], where N is the total number of carriers. Therefore, another parameter, defined as the ratio of $1/f$ noise normalized for bias, frequency and unit volume to resistivity (ρ), $K = C/\rho$ is used, even if N is unknown. It was originally introduced in [21] for layered materials as $K = C_{us}/R_{sh}$, where $C_{us} = C/d$ is the noise intensity normalized per unit area and $R_{sh} = \rho/d$ is the sheet resistance. The parameter K is widely used as a figure of merit for both homogeneous and inhomogeneous materials, even if they are made in different technologies. The obtained C-value and $\rho = 7.4 \cdot 10^{-3}$ Ωm for PTFRs studied in this work, lead to $K = 1.4 \cdot 10^{-7}$ μm$^2/\Omega$, which is a typical value for percolation in thick-film resistors and conductive polymers [18, 20, 22]. It is a well-known fact that the inhomogeneous electric fields and current crowding on a microscopic scale result in high K-values and apparent α_H (Hooge parameter) [22, 23]. It is in line with the conclusions given in [24], where exhaustive studies of electrical properties of polymer resistors with carbon black and/or graphite fillers, have been carried out and conduction as well as noise generation mechanisms have been explained within the framework of percolation theory. Furthermore, analysing the plot shown in Fig. 3a we may conclude that using the ac method the noise exploration is possible at a significantly smaller excitation magnitude comparing with that of a dc method. It is of great importance in low-temperature studies, in which preventing the sample from self-heating is the key issue [12].

Another interesting conclusion concerning noise sources in PTFRs is that the noise generation mechanism is linear, *i.e.* the dependence of noise intensities on both ac and dc excitation is the same, making points overlap each other in the plot of Fig. 3a. It is contrary to the nonlinear mechanisms that make the noise intensity for an ac excitation much smaller (even 2–3 decades) than that for a dc excitation [25, 26].

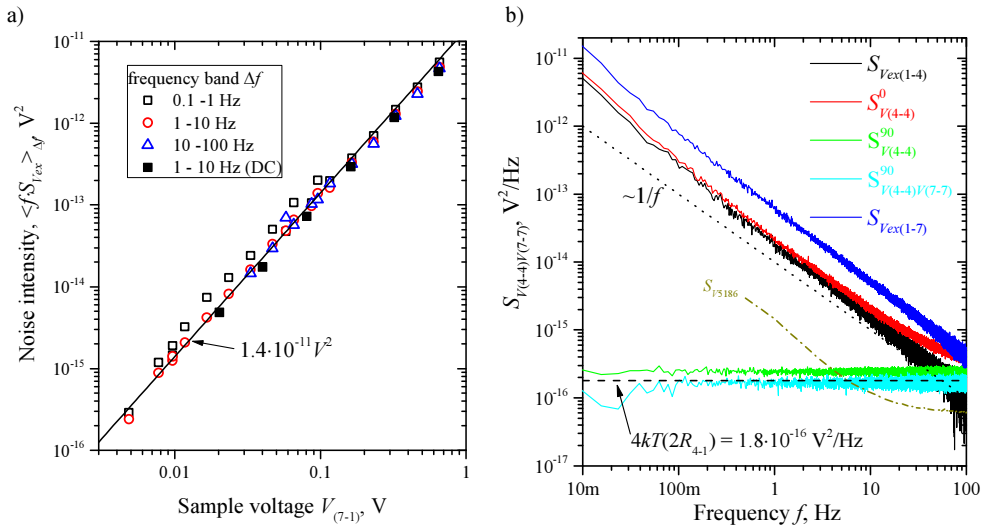

Fig. 3. a) The noise intensity as a function of the sample voltage in different frequency bands (open symbols) and the approximation for the frequency band 1–10 Hz with voltage square (line). The solid symbols, added for comparison, denote the data obtained in a dc method. b) The spectra obtained in different ways for the sectors 1–4 of the resistive layer at the sample voltage $V_{(7-1)} = 48$ mV, *i.e.* $V_{(4-1)} = 24$ mV. The dashed line indicating the thermal noise of the sectors (1–4) and the dotted line showing the pure $1/f$ noise as well as the amplifier noise S_{I5186} (dash-dotted line) have been added for reference.

5. Correlation method

An important advantage of the ac method is the possibility of exploration of noise spectra at the limit of extremely low frequency, limited only by the period of observation. Furthermore, the contribution of the amplifier noise in the ac method depends on the carrier frequency, a careful selection of which may minimize the contribution to S_V^{90}. It is worth to note, that for the 5186 amplifier, used in the studies, the power spectral density of its noise at 325 Hz is $1.7 \cdot 10^{-17}$ V^2/Hz (see Fig. 2) and sharply rises for frequencies below 10 Hz. However, a further reduction of the amplifier noise contribution is still possible, *e.g.* by the use of a correlation technique for S_{VV}^{90} measurements, *i.e.* calculating the cross-spectrum of signals detected at 90° in two independent signal paths. Next, expanding the concept by the use of a multi-terminal configuration of the sample in conjunction with the correlation method makes it possible to localize noise components originated in different parts of the multi-terminal device. For example, calculating the cross-spectra $S_{V(x-x)V(7-7)}^{0}$ and $S_{V(x-x)V(7-7)}^{90}$, where $V_{(7-7)}$ and $V_{(x-x)}$ are voltages taken from the bridge diagonal (terminals 7–7) and its sub-diagonal x–x, the excess noise $S_{Vex(1-x)}$ of the sectors of resistive layers, located between contacts 1 and x, may be obtained as:

$$S_{Vex(1-x)} = S_{V(x-x)V(7-7)}^{0} - S_{V(x-x)V(7-7)}^{90} \cdot \tag{4}$$

It is worth to note, that the method described by (2) could not be used in this case. The advantage of the above concept has been demonstrated in Fig. 3b where the spectra obtained in different ways have been gathered for comparison. Since the spectrum $S_{V(4-4)}^{90}$ was measured on the side-contacts, it includes – apart from the noise originated in the resistive layer located between side-contacts 1 and 4 – also the noise of voltage contacts. Therefore, $S_{V(4-4)}^{90}$ gives

the overestimated value of noise magnitude. On the contrary, the cross-spectrum $S^{90}_{V(4-4)V(7-7)}$ gives the correct value of thermal noise of sectors 1–4, evidencing usefulness of the correlation technique. The resistance $R_{(4-1)}$ = 5.5 kΩ, involved in calculation of the thermal noise $4kT(2R_{(4-1)}) = 1.8 \cdot 10^{-16}$ V²/Hz, has been measured using four-wire method, $R_{(4-1)} = V_{(4-1)}/I_{(7-1)}$, where $V_{(4-1)}$ is the voltage drop on terminals 1 and 4 measured under the current excitation $I_{(7-1)}$ flowing from contact 7 to contact 1. The excess noise $2\mathrm{Re}(S^{45}_{V(4-4)V(4-4)})$ and $S^{0}_{V(4-4)}$ measured directly on the sub-diagonal (4–4) also lead to overestimate the noise magnitude of sectors (1–4).

6. Noise suppression

During the noise exploration of PTFRs, it has been observed that the spectra of background noise, apart from those of white noise, contained also an unexpected $1/f$ component, whose intensity has been found to be strongly dependent on the carrier frequency. It has been shown in Fig. 4, where the spectra S^{90}_{V}, obtained at the fixed sample voltage of $V_{(7-1)}$ = 0.31 V and at different carrier frequencies, have been gathered. The excess noise component, $S^{90}_{Vex} = S^{90}_{V} - 4kT(2R_S)$, has been calculated and plotted in the inset. The explanation of the phenomenon is of great importance since S^{90}_{V} is involved in calculation of S_{Vex} (see (4)).

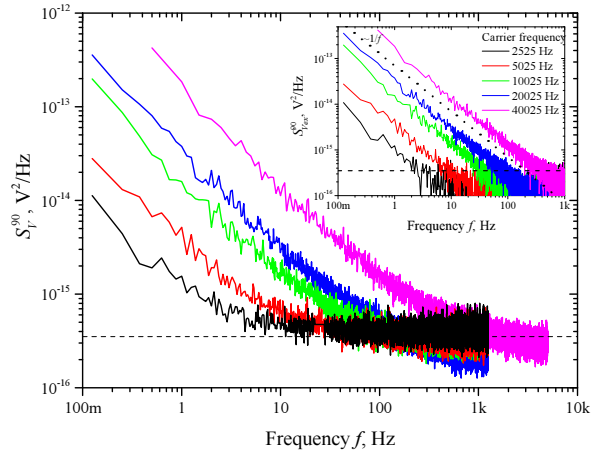

Fig. 4. The selected spectra of $S^{90}_{V(7-7)}$ for the sample voltage fixed at $V_{(7-1)}$ = 0.31 V and for different carrier frequencies. Inset: the excess noise component. The dashed line indicating the thermal noise of the samples and the dotted line showing the pure $1/f$ noise have been added for reference.

The analysis of the noise intensities, $s^0 = < fS^0_{Vex} >_{\Delta f}$, $s^{90} = < fS^{90}_{Vex} >_{\Delta f}$, plotted in Fig. 5a, reveals that both S^0_V and S^{90}_V components depend on the carrier frequency, although the dependence of S^{90}_V is more pronounced. The noise model for the bridge circuit of Fig. 1 is proposed in order to explain the observed dependence. The equivalent circuit consisting of (*i*) the ballast and sample resistances, (*ii*) the equivalent capacitance, C_{eq}, including the capacitance of the circuit, wire connecting the output voltage to the amplifier, the preamplifier input, and (*iii*) the noise source U_n, is shown in Fig. 5b. The circuit acts as an impedance voltage divider, yielding:

$$\frac{U_{amp}}{U_n} = \frac{1 - j2\pi f_{carrier}(R_B \parallel R_S)C_{eq}}{1 + \left[2\pi f_{carrier}(R_B \parallel R_S)C_{eq}\right]^2}, \tag{5}$$

where: $(R_B \parallel R_S)C_{eq}$ is the time constant of the circuit. Switching to power spectral densities, we arrive at:

$$\frac{S_V^0}{S_V^{90}} = \left[2\pi f_{carrier}(R_B \parallel R_S)C_{eq}\right]^{-2}. \tag{6}$$

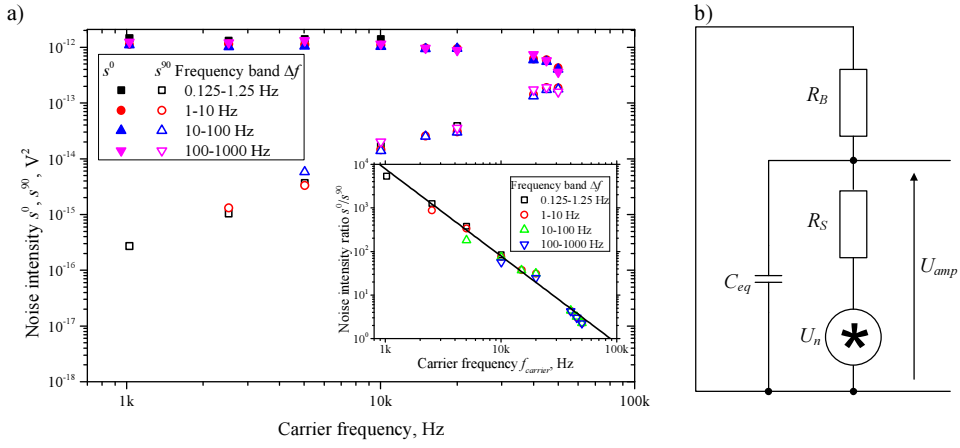

Fig. 5. a) The intensities of excess noise, calculated for S_V^0 (solid symbols) and S_V^{90} (open symbols) in different frequency bands, as a function of the carrier frequency. Inset: the noise intensity ratio (symbols) as a function of the carrier frequency. The line is the plot of r.h.s. of (6) with values of parameters given in the text. b) The noise model for the circuit of Fig. 1.

The comparison of the model prediction with the experimental data is shown in the inset of Fig. 5a, where the noise intensity ratio, s^0/s^{90}, calculated for different frequency bands is plotted as a function of the carrier frequency (open symbols). The solid line is the plot of r.h.s. of (6) for C_{eq} =180 pF, R_S = 11.12 kΩ, R_B = 100 kΩ, that were directly measured by the precision RLC meter (E4890A from Agilent), giving an excellent agreement with the experimental data in a wide range of carrier frequencies. Hence, we conclude that the observed $1/f$ component of S_V^{90} relates to a phase change of both in-phase and quadrature signal components, caused by impedances in the measurement circuit. The most significant contribution to the capacitance C_{eq} is the voltage transfer line (approx. 100 pF), indicating possible optimization of the circuit in order to minimize the analyzed effect. Another possibility of improvements in the properties of the ac bridge is replacing the variable resistor and the capacitor, used for balancing the bridge, with a simple low-noise resistor, and controlling the balance by the use of a two-channel sine waveform generator with precise programming of amplitude and phase coupling.

7. Conclusions

A method of noise measurements with the use of an ac excitation of the tested device has been developed. The progress in the technique is in using a multichannel daq module and software for multichannel phase sensitive detection instead of an expensive lock-in amplifier. In this way, it is possible to carry out the phase-sensitive detection for many signals at different sets of phase angles simultaneously, which is not possible when using a standard lock-in amplifier. The developed multichannel virtual lock-in technique has been shown to be helpful

for noise exploration in polymer thick-film resistors. The method has been verified with the use of (*i*) a traditional (stand-alone) lock-in amplifier for phase-sensitive detection and (*ii*) a typical dc method of noise measurement. All methods give consistent results. It has been confirmed that the $1/f$ noise caused by resistance fluctuations is the dominant noise component in PTFRs made of ED7100 resistive composition with Cu contacts. The value of noise parameter describing material noise intensity, $C = 1 \cdot 10^{-21}$ m^3, found in this work is in a good agreement with $8.2 \cdot 10^{-22}$ m^3 obtained with a dc method [17]. Furthermore, the parameter $K = 1.4 \cdot 10^{-7}$ μm^2/Ω is typical for percolation in thick-film resistors and conductive polymers. A very interesting observation was, that the background noise component obtained with the ac method includes an unexpected $1/f$ component. The phenomenon has been analysed and explained as the noise suppression by impedance of the measurement circuit, giving an excellent agreement with the experimental data. The multichannel VLI technique may replace hardware instruments, making the functionality more flexible and powerful. It is a very promising technique in noise characterization of low-ohmic samples and/or using an extremely low frequency which is outside the limit of a dc method. Moreover, using a multichannel daq-board, the noise signals from several pairs of sample terminals may be detected, which makes it possible to use the correlation method not only for reduction of system noise, but also for localization of noise sources in different parts of the resistor [27] and evaluation of the contact noise, giving information about the quality and interactions at the resistive/conductive layers' interface [18]. Experiments in which an ac method has been used in conjunction with a correlation technique are extremely rare due to the need of employing several expensive hardware lock-in amplifiers. We hope that the approach, described in the work, will break the barrier.

The developed VLI is easy to expand in order to increase its functionality, like *e.g.* evaluation of the 3rd (or any other) harmonic index [28, 29] which is also used for testing the reliability and quality of electronic components, instead of rather difficult noise measurements, as well as impedance analysis at the mHz-frequency range which is not available in the standard impedance analysers and meters. It has been also possible to use the ac method in exploration of the noise properties of nonlinear and other passive electronic components like capacitors and inductors. Furthermore, comparing noise intensity dependencies on dc and ac excitations we may recognize nonlinearity of conduction and/or noise generation mechanisms [25, 26].

Acknowledgements

The work has been supported from Grant DEC-2011/01/B/ST7/06564 funded by National Science Centre (Poland) and from statutory activity from Department of Electronics Fundamentals of Rzeszow University of Technology and Wroclaw University of Technology. Studies have been performed with the use of an equipment purchased in the project No POPW.01.03.00-18-012/09 from the Structural Funds, The Development of Eastern Poland Operational Programme co-financed by the European Union, the European Regional Development Fund.

References

[1] Directive 2002/95/EC of the European Parliament and of the Council of 27 Jan. 2003 on the restriction of the use of certain hazardous substances in electrical and electronic equipment.

[2] Kotadiaa, H.R., Howesb, P.D., Mannan, S.H. (2014). A review: On the development of low melting temperature Pb-free solders. *Microelecron Reliab.*, 54(6–7), 1253–1273.

[3] Busana, M.G., Prudenziati, M., Hormadaly, J. (2006). Microstructure development and electrical properties of RuO_2-based lead-free thick film resistors. *J. Mater. Sci. Mater. Electron.*, 17(11), 951–962.

[4] Hrovat, M., Kielbasinski, K., *et al.* (2012). The characterisation of lead-free thick-film resistors on different low temperature Co-fired ceramics substrates. *Mater. Res. Bull.*, 47(12), 4131–4136.

[5] Vandamme, L.K.J. (1994). Noise as a diagnostic tool for quality and reliability of electronic devices. *IEEE Transactions on Electron Devices*, 41(11), 2176–2187.

[6] Jevtić, M.M. (1995). Noise as a diagnostic and prediction tool in reliability physics. *Microelectron Reliab.*, 35(3), 455–77.

[7] Jevtić, M.M., Mrak, I., Stanimirović, Z. (1999). Thick-film resistor quality indictor based on noise index measurements. *Microelecron Reliab.*, 30(12), 1255–9.

[8] Rocak, D., Belavic, D., *et al.* (2001). Low-frequency noise of thick-film resistors as quality and reliability indicator. *Microelectron Reliab.*, 41(4), 531–42.

[9] Hasse, L.Z., Babicz, S., Kaczmarek, L., Smulko, J.M., Sedlakova, V. (2014). Quality assessment of ZnO-based varistors by 1/*f* noise. *Microelectron Reliab.*, 54(1), 192–199.

[10] Stadler, A.W., Kolek, A., Mleczko, K., Zawiślak, Z, Dziedzic, A., Nowak, D. (2015). Noise properties of thick-film conducting lines for integrated inductors. *Metrol. Meas. Syst.*, 22(2), 229–240.

[11] Scofield, J.H. (1987). ac method for measuring low-frequency resistance fluctuation spectra. *Rev. Sci. Instrum.*, 58(6), 985–93.

[12] Ptak, P., Kolek, A., Zawiślak, Z., Stadler, A.W., Mleczko, K. (2005). Noise resolution of RuO_2-based resistance thermometers. *Rev. Sci. Instrum.*, 76(1), 014901.

[13] Verbruggen, A.H., Stoll, H., Heeck, K., Koch, R.H. (1989). A novel technique for measuring resistance fluctuations independently of background noise. *Applied Physics A*, 48(3), 233–236.

[14] Trabjerg, I., Hansen, T. (1998). Photoacoustic powder spectra of Ni(II) and Co(II) complexes with aromatic amine *N*-oxide ligands. *Spectrochim. Acta Mol. Biomol. Spectrosc.*, 54(11), 1715–1720.

[15] Gu, M., Wang, J.L., Zhang X. (2009). Thermal-Conductivity Measurements of Polymers by a Modified 3ω Technique. *Int. J. Thermophys.*, 30(3), 851–861.

[16] Lu, J., Pan, D.A., Yang, B., Qiao, L.L. (2008). Wideband magnetoelectric measurement system with the application of a virtual multi-channel lock-in amplifier. *Meas. Sci. Technol.*, 19(4), 045702.

[17] Stadler, A.W., Dziedzic, A. (2015). Virtual instruments in low-frequency noise spectroscopy experiments. *Facta Universitatis. Series: Electronics and Energetics.* 28(1), 17–28.

[18] Stadler, A.W. (2013). Fluctuating phenomena in resistive materials and devices. *Proc. Electron Technology Conference 2013*, *Proc. of SPIE 8902*, 890222.

[19] Hooge, F.N. (1990). The relation between 1/*f* noise and number of electrons. *Physica B*, 162(3), 344–352.

[20] Vandamme, L.K.J. (2013). How useful is Hooge's empirical relation. *Proc. of 22nd International Conference on Noise and Fluctuations (ICNF)*, Montpellier 2013, 1–6.

[21] Vandamme, L.K.J., Casier, H.J. (2004), The 1/*f* noise versus sheet resistance in poly-Si is similar to poly-SiGe resistors and Au-layers. *Proc. of the 34th European Solid-State Device Research Conference*, 365–368.

[22] Vandamme, L.K.J. (2011). Characterization of contact interface, film sheet resistance and 1/*f* noise with circular contacts. *Fluctuation and Noise Letters*, 10(4), 467–484.

[23] Vandamme, L.K.J., Trefan, G. (2002). 1/*f* noise in homogeneous and inhomogeneous media. *IEE Proc. Circuits Devices and Systems*, 149(1), 3–12.

[24] Dziedzic, A., Kolek, A. (1998). 1/*f* noise in polymer thick-film resistors. *J. Phys. D: Appl. Phys.*, 31(17), 2091–2097.

[25] van Helvoort, G.J.M., Beck, H.G.E. (1977). Model for the excitation of 1/*f* noise by high-frequency a.c. signals. *Electronics Letters*, 13(18), 542–544.

[26] Kolek, A. (2006). *Experimental methods of low-frequency noise*. Rzeszów: Rzeszow University of Technology – Publishing House.

[27] Kolek, A., Stadler, A.W., Zawiślak, Z., Mleczko, K., Dziedzic, A. (2008). Noise and switching phenomena in thick-film resistors. *J. Phys. D: Appl. Phys.*, 41(2), 025303 (1–12).

[28] Hasse, L., Smulko, J. (2008). Quality assessment of high voltage varistors by third harmonic index. *Metrol. Meas. Syst.*, 15(1), 23–31.

[29] Jóźwiak, K., Smulko, J. (2008). Methods of quality characterization of foil-based capacitors. *Metrol. Meas. Syst.*, 15, 305–316.